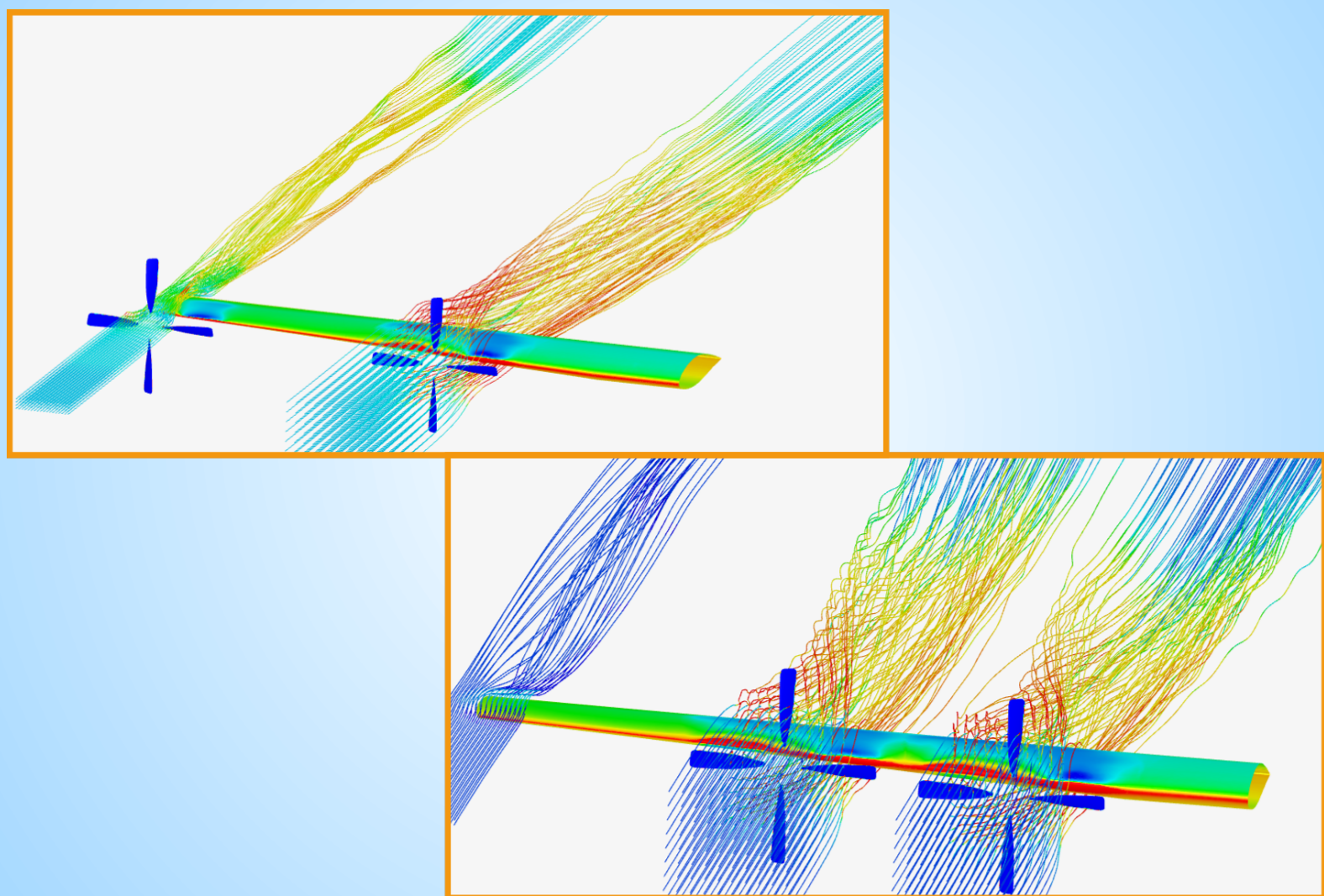


A Comprehensive CFD Study of the C130 Aircraft Wing: Winglet Effects and Propeller-Wing interaction Analysis



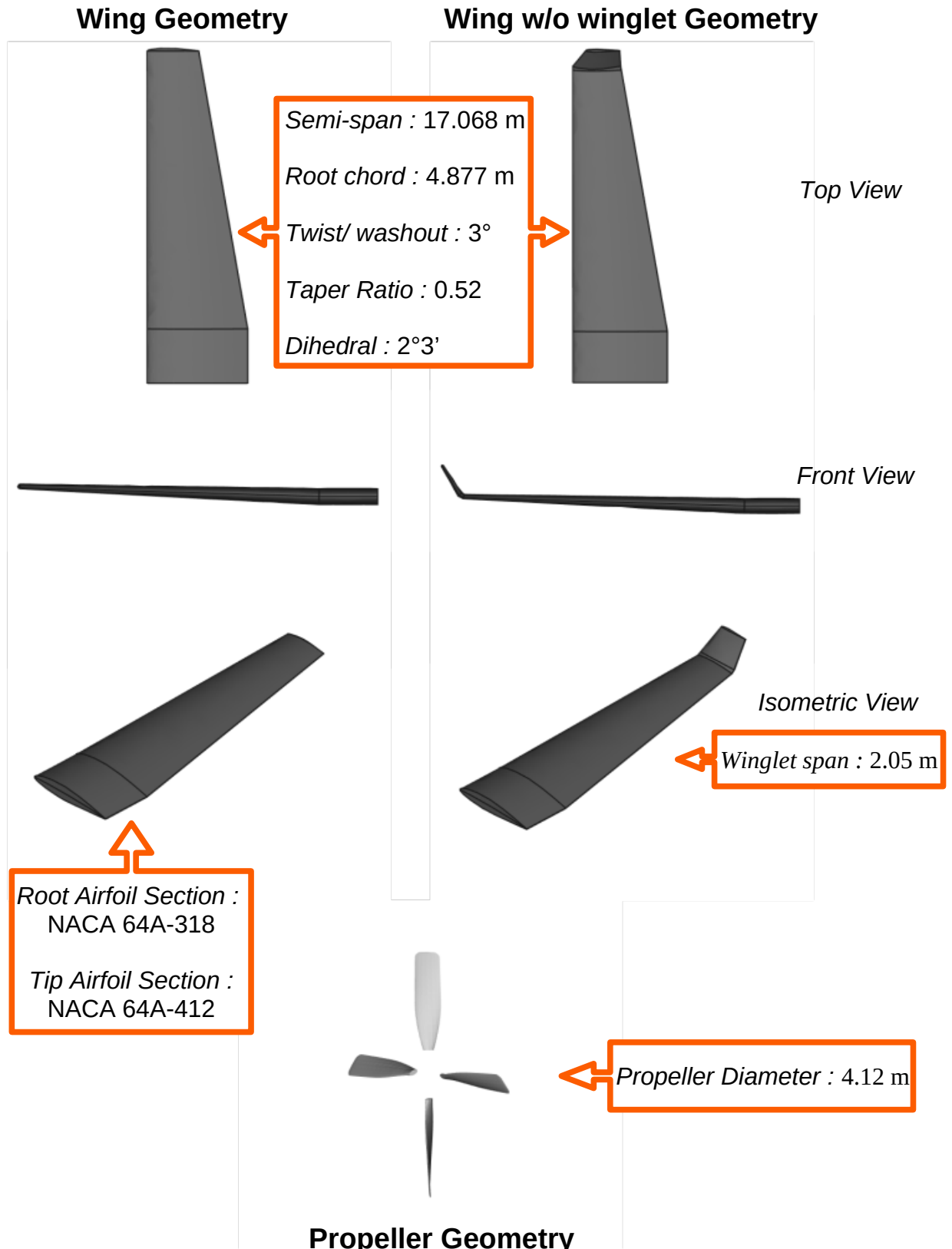
By-
Shantesh Rai

This project is divided into three sub-projects. The titles of all three parts are listed below:

- I. CFD Analysis of C130 Aircraft Wing: The Winglet Effect**
- II. A CFD Analysis of Wing-Propeller Interaction in C130 Aircraft**
- III. Enhancing Aerodynamic Efficiency of a Wing: Winglet v/s Wingtip-Propeller**

3D CAD Models

CAD modelling was done with open-source software OpenVSP.



CFD Analysis of C130 Aircraft Wing: The Winglet Effect

Introduction

The objective of this part of the project is to analyse and compare the aerodynamic performance of a wing with and without a winglet.

Winglets are small, vertical extensions at the tips of aircraft wings. Their primary purpose is to reduce induced drag, which occurs due to the generation of lift. A typical winglet design has following properties:

- Airfoil Shape: Winglets typically have an airfoil shape, similar to the main wing. The choice of airfoil affects their performance.
- Height and Angle: The height (or span) and angle of winglets are critical. They should be optimized based on the specific aircraft and its operating conditions.
- Attachment: Winglets are attached to the wingtip, either as an integral part of the wing or as separate add-ons.

The main advantages of adding a winglet to the wing are as follows:

- Reduced Induced Drag: Winglets decrease the vortices formed at the wingtips during flight. These vortices create induced drag, which winglets mitigate.
- Improved Fuel Efficiency: By reducing drag, winglets enhance fuel efficiency, especially during long flights.
- Increased Range: Longer flights are possible due to reduced fuel consumption.
- Better Climb Performance: Winglets improve climb rates by minimizing drag during ascent.
- Enhanced Stability: They contribute to lateral stability and dampen roll oscillations.

However, there are some disadvantages that come with them and that makes winglet design optimization imperative. Following are their potential drawbacks:

- Parasite Drag: Winglets increase the surface area exposed to airflow, leading to a slight increase in parasite drag (drag not related to lift).
- Added Weight: The weight of winglets impacts overall aircraft weight. However, this trade-off is usually acceptable.
- Structural Modifications: Retrofitting winglets to older designs may require structural changes to accommodate them.

CFD Modelling and Simulation Setup

The CFD modelling and simulations were carried out on the *Simscale* Platform. Figure 1 shows the computational domain of the simulations carried out for both the plain wing and winglet-wing. Different boundary conditions are highlighted. The table below enlists all the parameters used for simulation setup. Inflation layers were added on the wing surface to keep $y^+ < 3$.

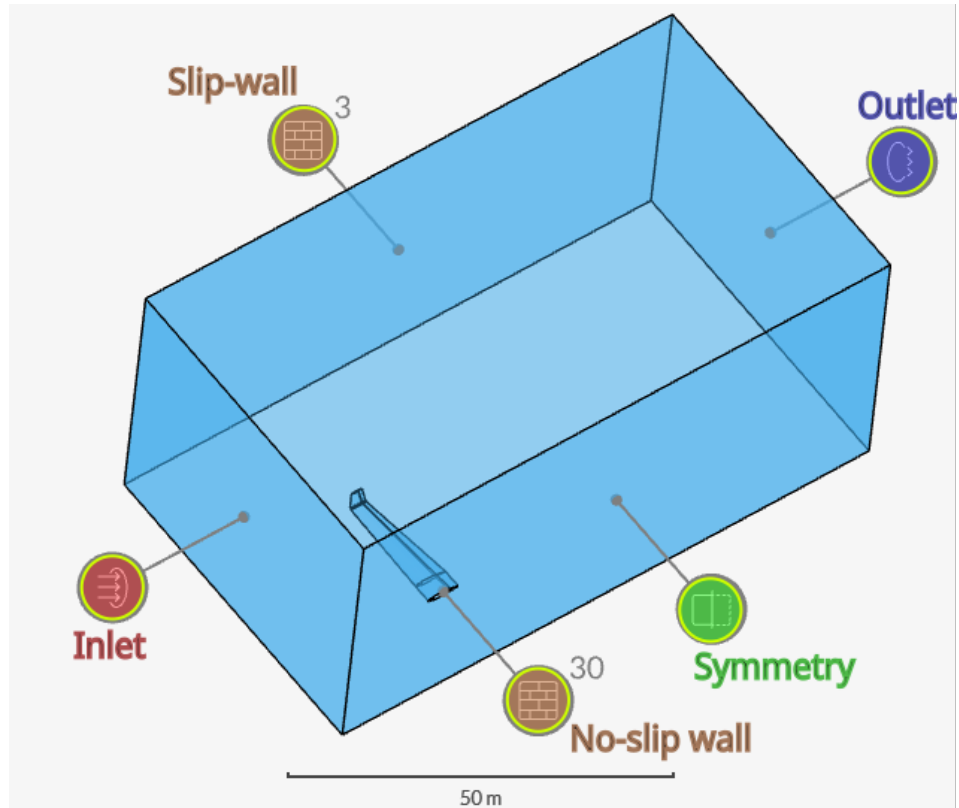


Figure 1: Simulation Domain

Angle of attack	3°
Inlet velocity [m/s]	66.9
Flight altitude [ft]	1000
Atmospheric Pressure [Pa]	97666.4
Air kinematic viscosity [m ² /s]	0.0000148
Air density [kg/m ³]	1.196
Time dependency	Steady-state
Turbulence model	k- ω SST
No. of volume cells (plain-wing)	5700993
No. of volume cells (winglet-wing)	5852390

Results and Discussion

Wingtip Flow Visualization:

Figure below depicts the flow streamlines at the wingtips. Vortex formation can be seen in the flow for the plain wing. This happens when high-pressure air from below the wing leaks into the low-pressure region above the wing around the wingtips. A dramatic decrease in the vortex formation can be seen, when a winglet is added to the wing.

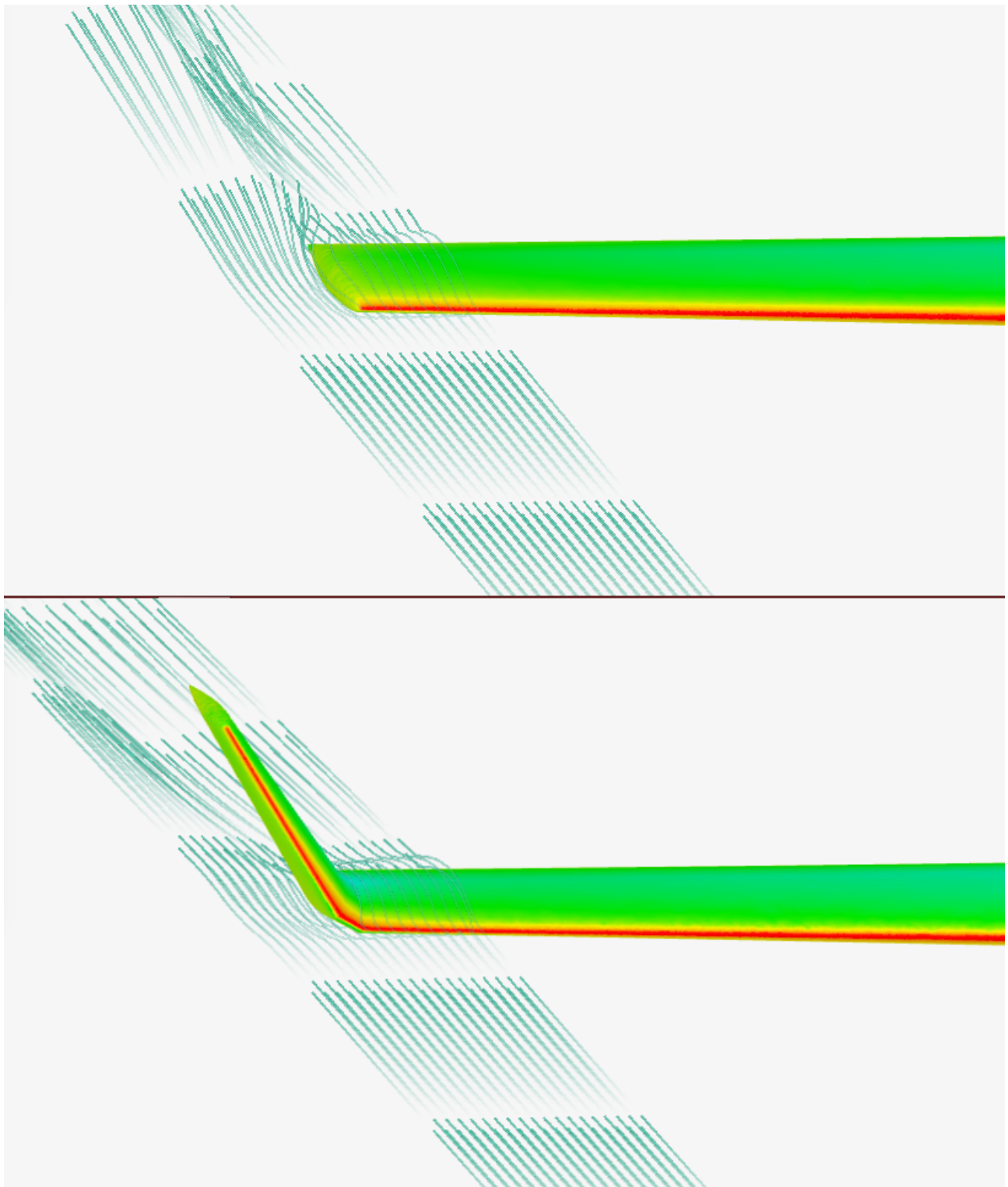


Figure 2: Flow Streamlines at the Wingtip of plain wing (above) and winglet-wing (below)

These vortex formation not only affect the wingtip region but also the entire wingspan and wake region. The vortices lead to a circulating mass of air in the surrounding region as well as behind the wing. The swirling air, particularly behind the wing, induces a downward directed airflow leading to, what is called a downwash.

Due to this downwash, the relative airflow approaching the wing is no longer horizontal but slightly tilted downward. Consequently, the lift vector, which is perpendicular to the airflow, tilts backward. The vertical component of this new lift vector acts as a reduced lift force and the horizontal component results in an induced drag.

The induced drag is more pronounced at lower operating speeds, such as during take-off and landing. During these stages, to compensate for lower speeds the angle-of-attack is increased so that more lift is generated. As a consequence, the pressure difference between the upper and lower wing surface increases, which makes vortices stronger leading to more downwash and induced drag.

A winglet acts as a barrier that inhibits the airflow around the wingtip. This weakens the vortices and reduces downwash, thereby decreasing induced drag. Not only this, since the airflow is redirected by the winglet, some of the energy is recaptured and added towards the lift force which would otherwise be lost in the vortex formation. Overall, a well-designed winglet would increase the aerodynamic efficiency of the wing, saving fuel and cost.

Coefficient of Pressure (C_p):

The figure below shows the distribution of coefficient-of-pressure (C_p) over the top and bottom surface of both wings. The C_p is a dimensionless number that describes the relative pressure at a point on a surface with respect to the freestream (ambient) pressure of the surrounding fluid. It is used as a representation of how the lift is distributed over the wing surface.

On the top surface, C_p values are mostly negative while it is positive on most part of the lower surface for both wings. This indicates that the wing is producing lift. From the wing root to the mid-wing, the C_p values on top surface have slightly decreased for the winglet-wing when compared to the plain-wing. From mid-wing to wingtip, there is a significant decrease in C_p values on the top surface of the winglet-wing in contrast to the plain-wing.

These observations corroborates with the theory in the previous section. The winglet helps in reducing the downwash and also redirects the airflow at the wingtips, thereby, recovering the lift force that was lost to the induced drag and vortex formation. In addition, the winglet surface also generates lift force as seen in the figure 3 below.

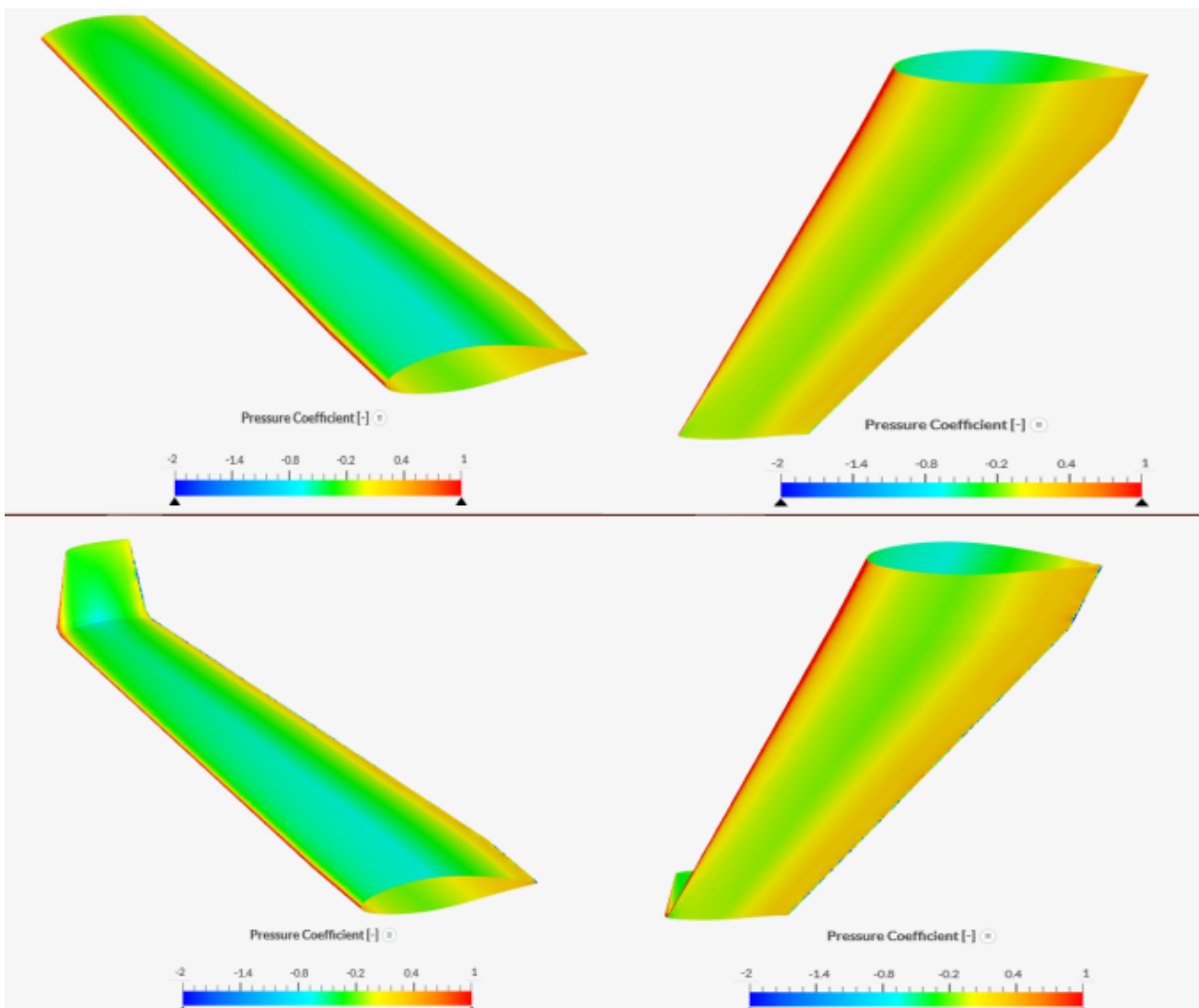


Figure 3: Pressure coefficient distributions over upper and lower wing surface of plain wing (top) and winglet-wing (bottom)

Vorticity and Wake Velocity:

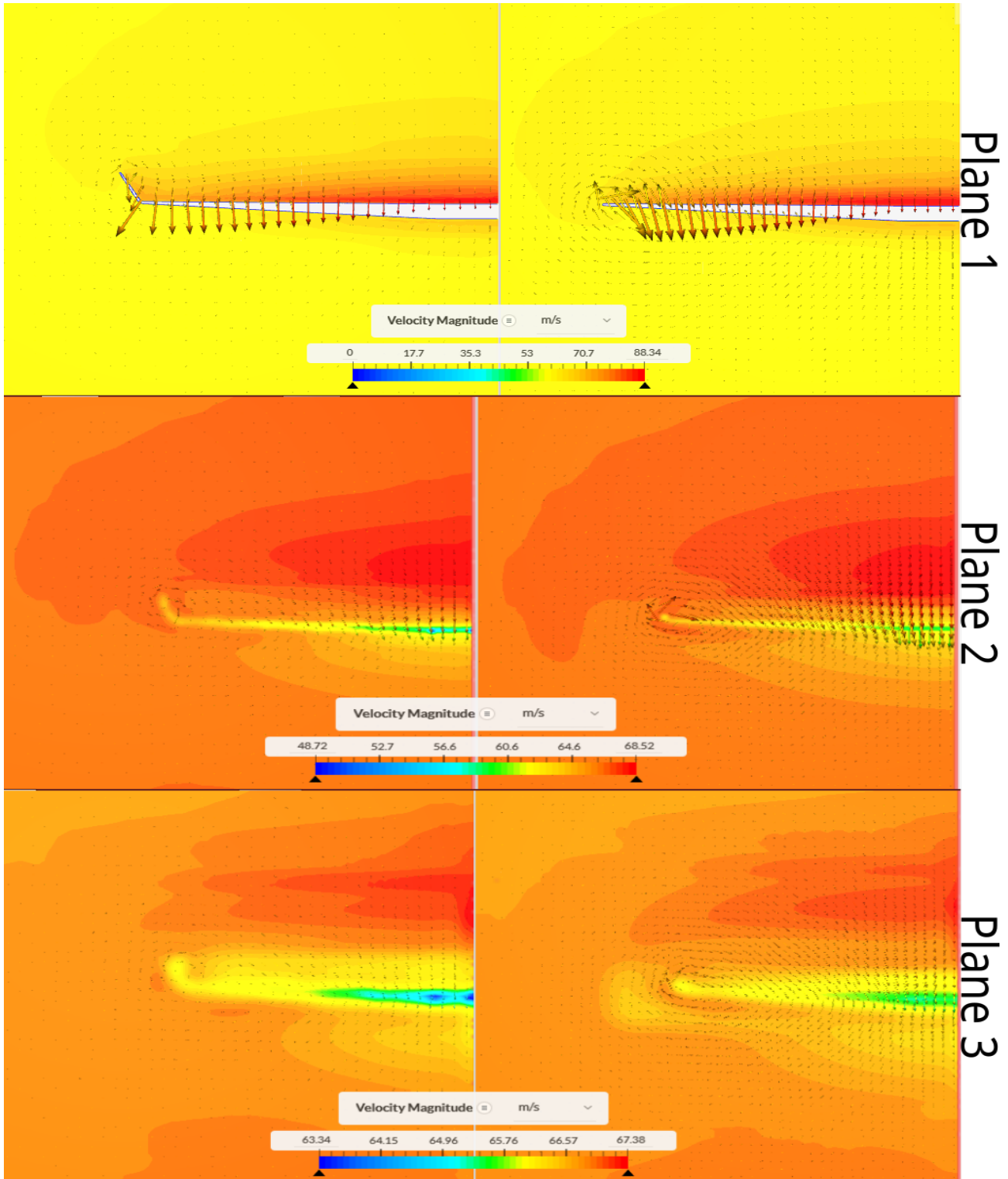


Figure 4: Velocity contours plotted at three locations along the airflow direction for plain-wing (right column) and winglet-wing (left column)

In the figure above, velocity contours are plotted at three different locations along the airflow direction viz. 1.93 m (Plane 1), 5.64 m (Plane 2), and 9 m (Plane 3) from the leading edge of the wing. The maximum and minimum velocity values are determined and used as the scale range for each plane to analyse the velocity distribution and vortex formation in

the wake region.

Plane 1 is located almost at the midpoint on the chord line. The maximum velocity is similar for both wings. However, due to the presence of the winglet, more region of air has a higher velocity than the freestream velocity of 66.9 m/s in the winglet-wing case. Moreover, the velocity vectors show a stronger vortex formation at the wingtip of the plain-wing.

Plane 2 and 3 are located in the wake of the wings. The wake of the winglet-wing has regions of much lower velocity than that of the plain-wing. For the plain-wing, it is ostensible that the low velocity air and high velocity air leaks into opposite region around the wingtip. While this is not the case for winglet-wing. The velocity vectors again show a stronger vortex formation in the wake of the plain-wing than that of the winglet-wing.

Lift, Drag and Efficiency:

	Lift force (L) [N]	Drag force (D) [N]	Efficiency (L/D)
Plain-wing	79433.92	4564.71	17.4
Winglet-wing	84080.09 (+5.85%)	6576.17 (+44.07%)	12.79 (-26.5%)

The lift and drag force values of the last 50 iterations were averaged-out and tabulated above. Agreeing with the theory discussed in previous sections, the lift shows an increment of 5.85% when the winglet was added. However, the drag force also increased sharply by 44.07% for the winglet-wing when compared with the plain-wing. Consequently, the aerodynamic efficiency of the winglet-wing is reduced by 26.5% when compared with the plain-wing.

The results for aerodynamic efficiency seem like an antithesis of the theoretical effects of a winglet as discussed above. This can be explained by dividing the total drag force into two types, namely parasitic drag and induced drag. Induced drag was explained in the previous section. Parasitic drag on the other hand, is the result of form drag and skin friction (viscous) drag. At low speed, such as during take-off and landing, the induced drag is the major contributor due to high angle of attack. At high speed, such as during cruise condition, the parasitic drag becomes the dominant type and induced drag is very small.

In this project, the wing is in cruise condition with a small angle of attack. Ergo, a winglet's effect on induced drag will not have a significant improvement in aerodynamic efficiency of the wing. On the contrary, the increase in wing surface area due to the winglet will increase the dominant parasitic drag, as is evident in the table above.

This is where the process of winglet design optimization comes into play. An unoptimized winglet can negatively impact the aerodynamic efficiency of the wing during cruise. This could be the potential reason behind the unexpected simulation result in this project.

Winglet Design Optimization

To test the hypothesis, the winglet design was modified while keeping the same airfoil section. The simulation domain, mesh settings and size as well as the simulation setup was kept same as before.

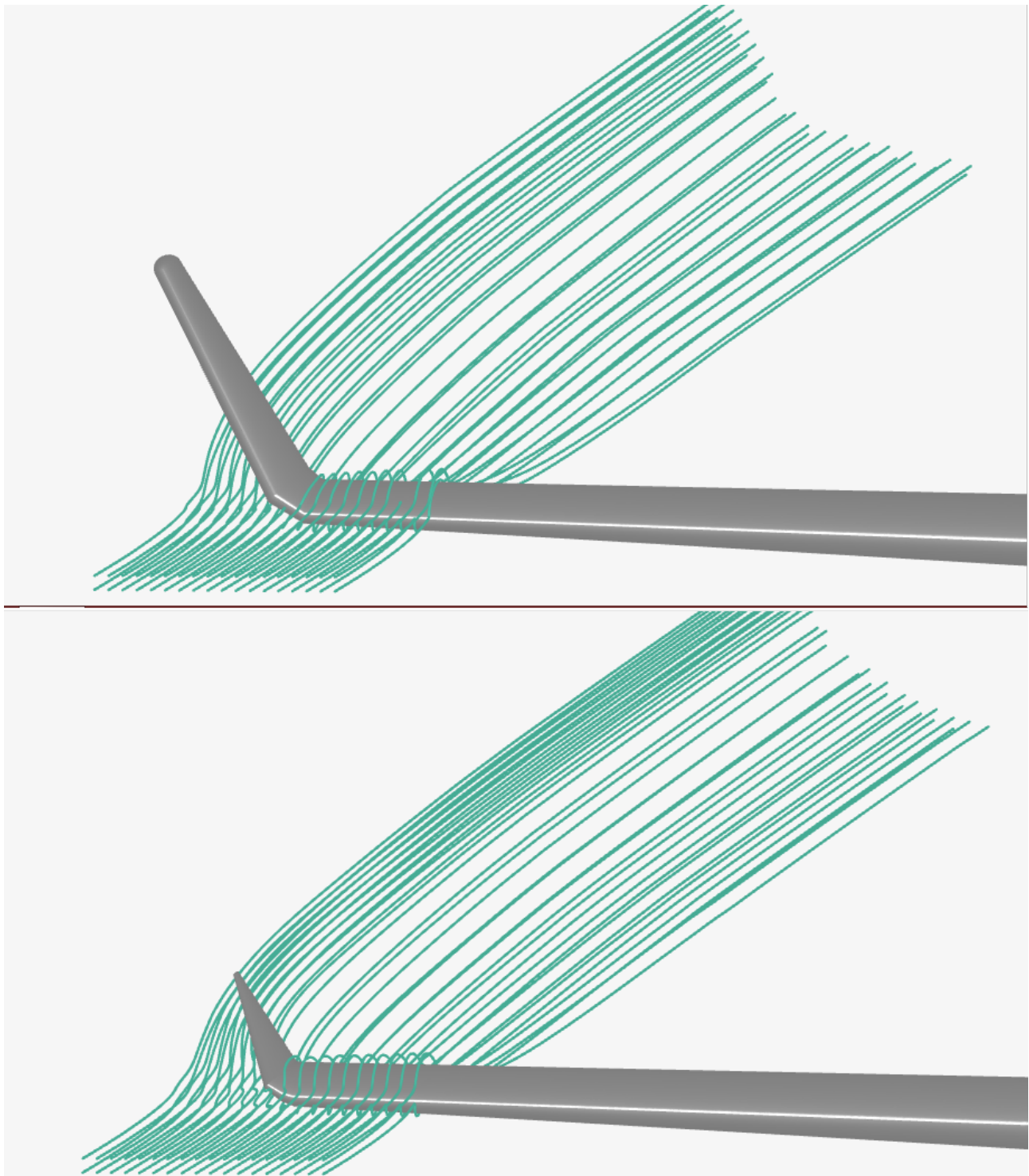


Figure 5: Flow streamlines for the original winglet-wing (top) and modified winglet-wing (down)

Figure above visualize the flow streamlines at the wingtip area for the original winglet

design as well as the modified winglet design. Both winglet designs seem to be effective in reducing the vortex formation at the wingtip.

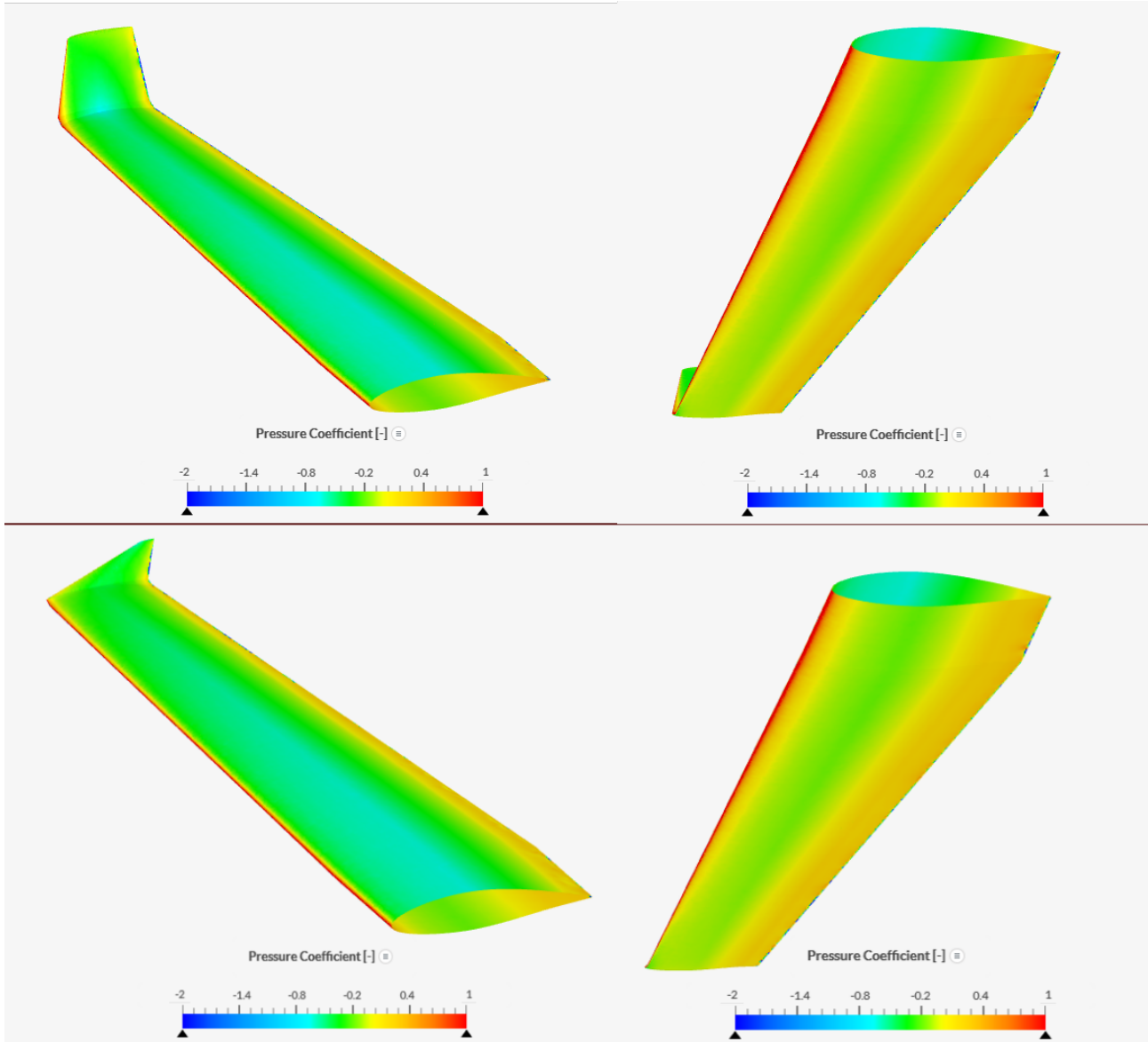


Figure 6: Pressure coefficient distributions over upper and lower wing surface of original winglet-wing (top) and modified winglet-wing (bottom)

Figure 6 shows the C_P distributions around the wing for both winglet designs. The distribution seems to be pretty much same for most of the wing-span, except for the wingtip region. Near the wingtip, the modified version seems to create less lift. Also, the winglet itself seems to generate less lift force for the modified winglet version.

	Lift force (L) [N]	Drag force (D) [N]	Efficiency (L/D)
Winglet-wing	84080.09	6576.17	12.79
Modified Winglet-wing	76500.95 (-9.01%)	5460.35 (-16.97%)	14.01 (9.54%)

Table above shows the average values of lift and drag forces over the last 50 iterations. The results show agreement with the hypothesis. The modified design shows an improvement of

9.54% in its aerodynamic efficiency when compared to the original winglet-wing design. This establishes the importance of winglet design optimization, which is a separate topic of study in its own. However, when compared to the plain wing, the aerodynamic efficiency of this new modified winglet-wing is still much lower. Moreover, this modified winglet-wing generates less lift force than the plain wing. So it is safe to say that more design optimization needs to be done.

A CFD Analysis of Wing-Propeller Interaction in C130 Aircraft

Introduction

Propeller planes remain crucial in modern and future aviation due to their efficiency on short-haul routes, lower operating costs, and ability to operate on shorter runways, making them ideal for regional flights and in areas with limited infrastructure. Their versatility, environmental benefits, and suitability for specialized missions further emphasize their importance. Studying wing-propeller interaction is vital for optimizing aerodynamic efficiency, reducing noise, enhancing stability and control, and addressing propeller-induced vibrations. This research is increasingly relevant with the rise of electric and hybrid-electric aircraft, where distributed propulsion systems rely on well-understood wing-propeller dynamics to improve performance and sustainability.

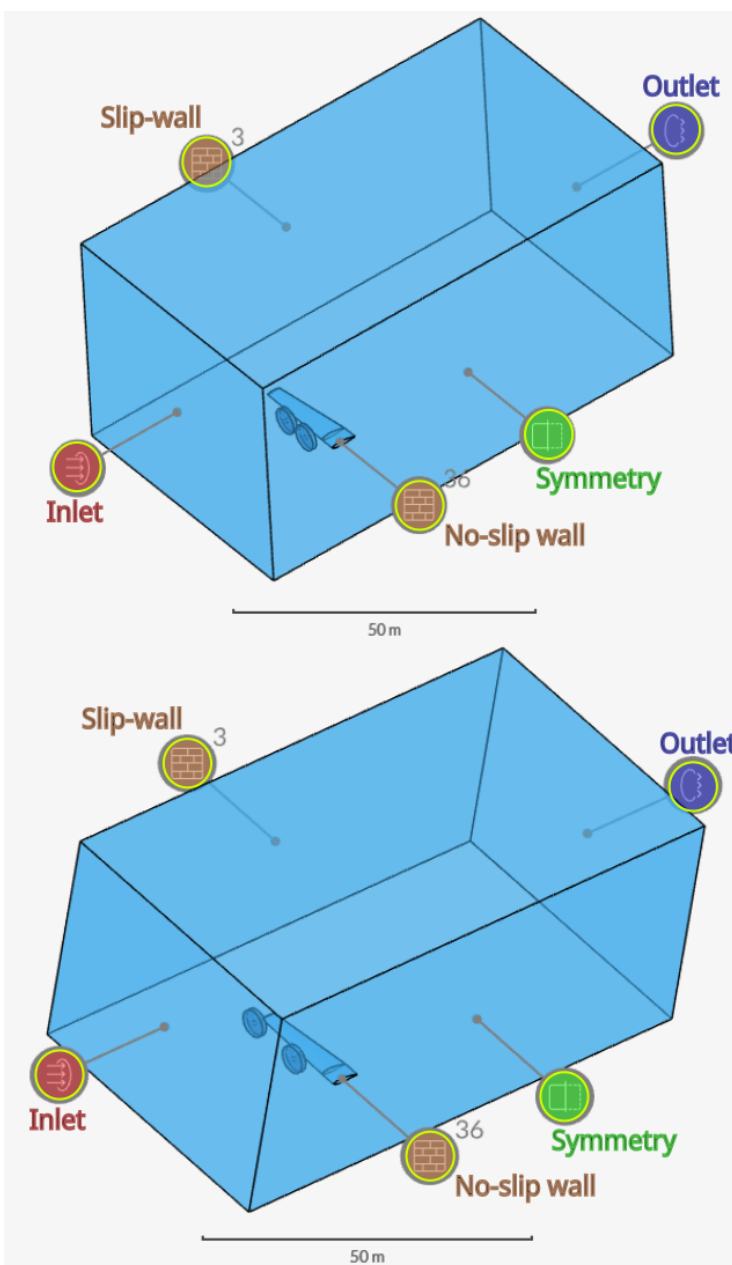
Specifically for the electric propulsion aircraft, the relatively light-weight and compact electric motors enables unconventional placement of propellers along the wing span. One such concept is that of the distributed propulsion. In a general sense, it refers to the use of many small-sized propellers distributed along the entire wing span. One of the reason behind the conception of distributed propulsion is to leverage the positive effects of wing-propeller aerodynamic interference along the entire wing span. Within this broad concept, the specific configuration of wingtip mounted propeller is of great interest due to its high potential of increasing the aerodynamic efficiency of the wing.

Wingtip propellers, mounted at or near the wingtips of an aircraft, are a critical component in modern and future aviation due to their ability to enhance aerodynamic efficiency by reducing induced drag and improving the lift-to-drag ratio. By counteracting wingtip vortices, these propellers lower fuel consumption and emissions, making them environmentally beneficial and cost-effective. They are particularly significant in distributed propulsion systems, especially in electric and hybrid-electric aircraft, where their contribution to optimized thrust and control enhances overall performance. Additionally, wingtip propellers can improve maneuverability, reduce noise, and decrease the wing bending moment, allowing for lighter, more efficient aircraft designs. Their role is pivotal in advancing sustainable aviation technologies, revolutionizing aircraft design, and supporting applications such as urban air mobility (UAM) and military surveillance, where efficiency, control, and reduced environmental impact are paramount.

With these trends in mind, the objective of this part of the project is to perform a CFD simulation of the aerodynamic interaction between the C130 aircraft wing and a propeller slipstream and analyse the outcomes for standard C130 propeller configuration and a concept wingtip-mounted propeller configuration.

CFD Modelling and Simulation Setup

The simulation modelling, setup and calculations were performed on the *Simscale* platform. Figure below shows the simulation domain for two propeller configurations. The top domain is of the standard C130 propeller configuration while the bottom one is of the wingtip propeller configuration. To adhere to the computational resource constraints, only wing and propeller blades are modelled. The propeller motion will be simulated using the AMI rotating zone. For this, the propellers are placed inside separate cylindrical zones of appropriate dimensions, as seen in the figure. The simulation is modelled for cruise condition. All the boundary conditions are represented in the figure. The table below enlists all the parameters used for simulation setup. Inflation layers were added on the wing and propeller blades to keep $y^+ < 3$.



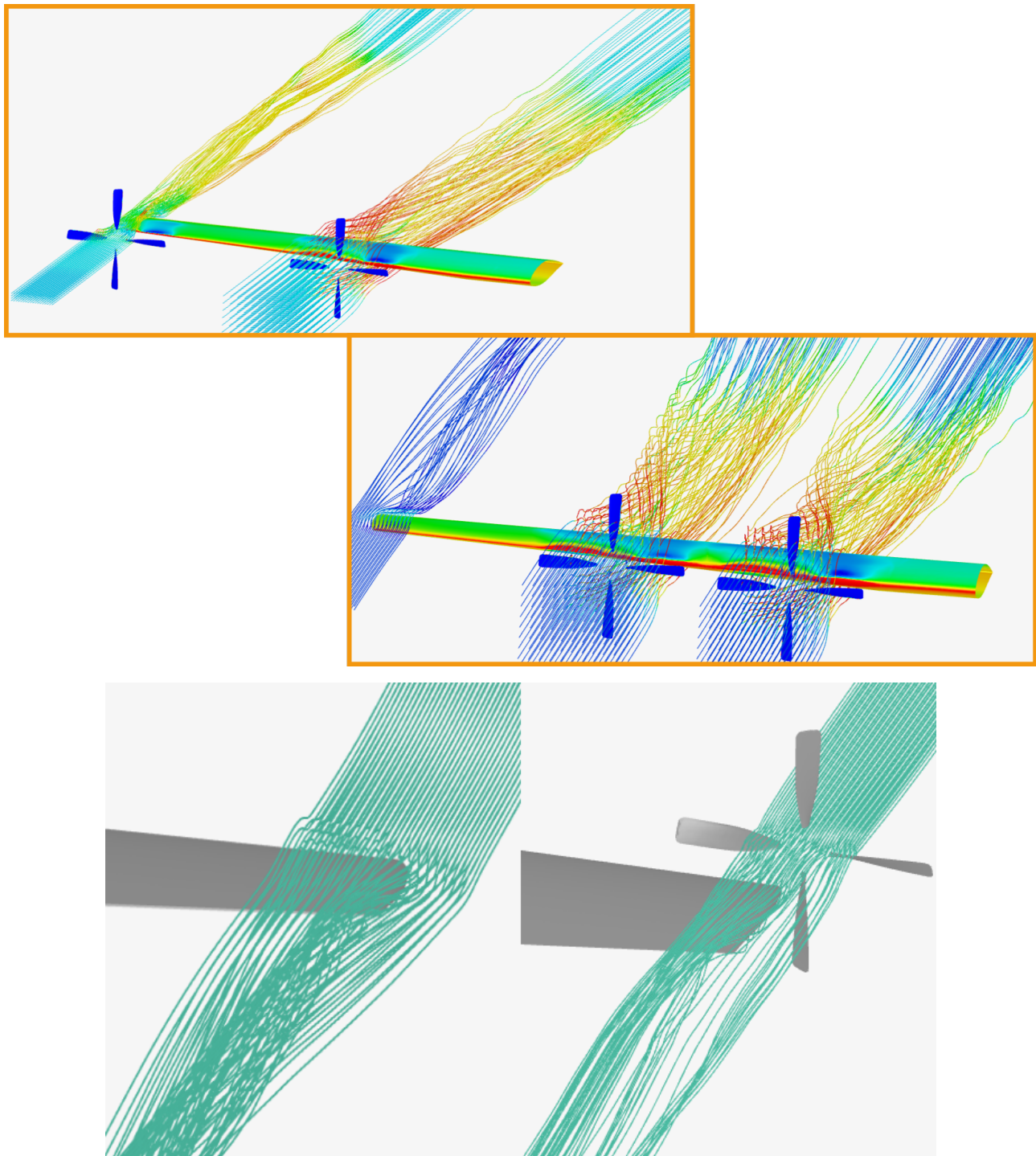
Angle of attack	3°
Inlet velocity [m/s]	66.9
Flight altitude [ft]	1000
Propeller rotational velocity [RPM]	1020
Atmospheric Pressure [Pa]	97666.4
Air kinematic viscosity [m ² /s]	0.0000148
Air density [kg/m ³]	1.196
Time dependency	Transient
Turbulence model	k- ω SST
No. of volume cells (standard config.)	7493611
No. of volume cells (wingtip config.)	7456105

Figure 7: Simulation Domain for Propeller-Wing in standard configuration (top) and wingtip configuration (bottom)

Results and Discussion

The simulations were run with a time-step size of 0.0001s for 5000 steps. The results below were taken from the last step at 0.5 sec.

Flow Streamlines Visualization:



Figures above show the flow streamlines for both configurations. The propellers are rotating in the anti-clockwise direction when viewed from the front of the wing. The area of particular interest here is the wingtip region. When the propellers are mounted in standard configuration, the airflow around the wingtip is same as that of a plain-wing (discussed in

the previous part of this project). This suggests strong vortex formation at the wingtip and induced drag, as is also evident in the figures above. However for the wingtip propeller configuration, a significant reduction in vortex formation can be seen. The anti-clockwise rotation of the propeller directly counters the vortex direction.

As discussed in the previous part of this project, wingtip vortices are directly connected to the induced drag on the wing. A reduction in vortex strength, therefore, reduces total drag acting on the wing. This indeed improves the aerodynamic efficiency of the wing i.e lift-to-drag ratio and reduces fuel consumption.

Propeller Performance:

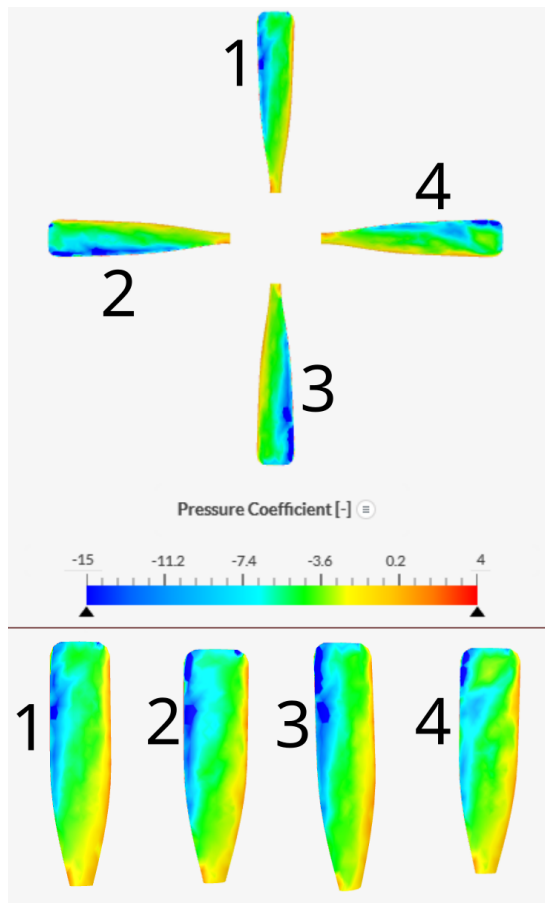


Figure 8: Pressure coefficient distribution on the propeller blades

Figure 8 above shows the distribution of pressure coefficient over the propeller blades. The presence of the wing in the slipstream of the propeller has two effects. First, there is an upwash near the leading edge of the wing and second presence of the wing reduces the slipstream velocity as it provides resistance to airflow.

Due to the upwash, the descending blades experience a slight increase in the angle-of-attack and the ascending ones experience a slight decrease. This causes an asymmetric distribution

of thrust in the propeller, which would otherwise be symmetric for an isolated propeller. The blades moving downward have higher thrust than the blades moving upward. The maximum thrust is produced at the lowest position blade. In the figure, propeller has a counter-clockwise rotation. Blade 3, therefore, shows the maximum thrust followed by blade 2 which is moving downward. Blade 4 has the least amount of thrust, as expected. These asymmetric blade thrusts lead to asymmetric relocation of the propeller's centre of thrust, called as P-factor.

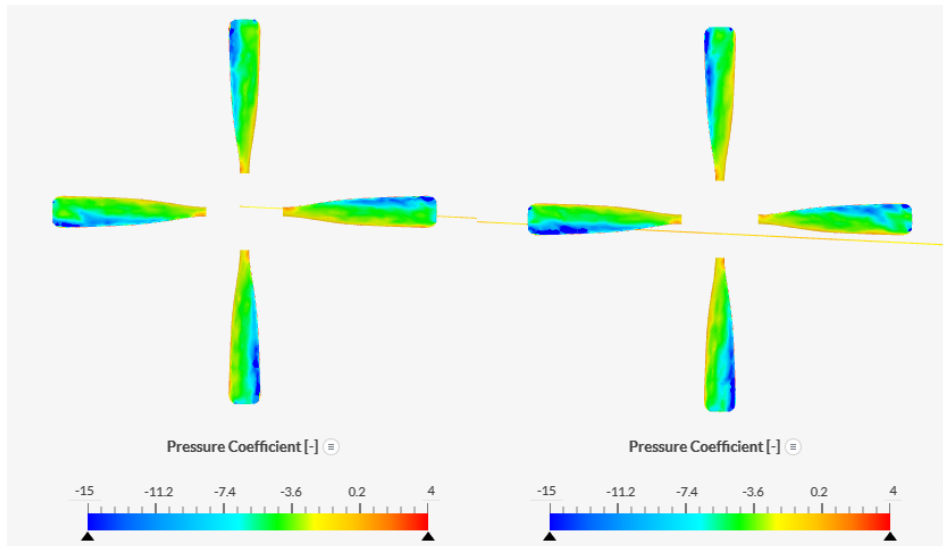


Figure 9: Pressure coefficient distribution on wingtip propeller (left) and inboard propeller (right)

Figure 9 contrasts the thrust generation on the wingtip-mounted propeller and the inboard propeller. While the wing upwash is present on both the sides of the propeller hub for the inboard propeller, it is present only on the right side of the hub for the wingtip propeller. Due to this, there is a decrease in the generated thrust for the wingtip propeller case. This ultimately reduces the propeller efficiency of the wingtip propeller in contrast to that of the inboard propeller.

Wing and Propeller-Slipstream Interaction:

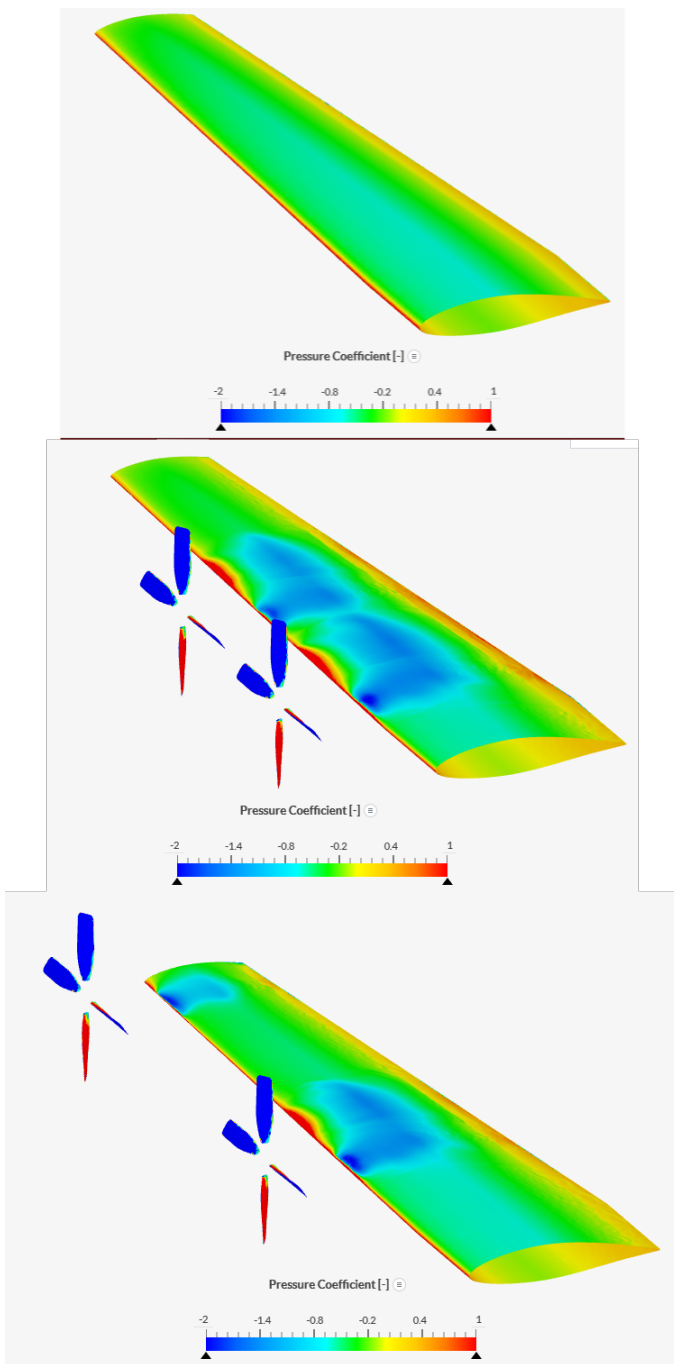


Figure 11: Pressure coefficient distributions over upper wing surface

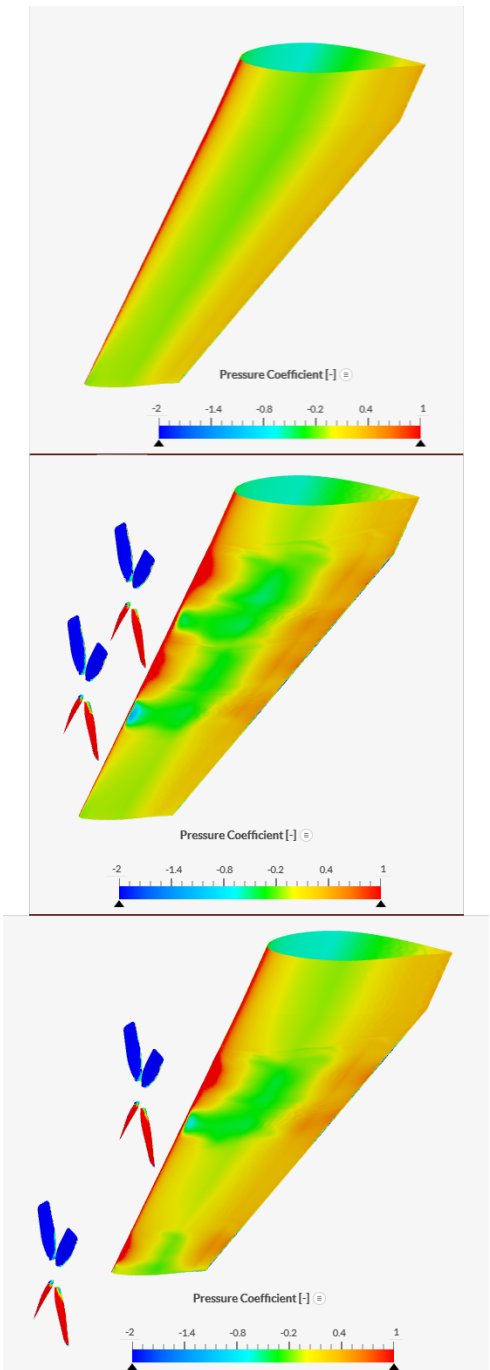


Figure 10: Pressure coefficient distributions over lower wing surface

Figures 10 and 11 depicts the distribution of pressure coefficient over the lower and upper surfaces of the plain-wing, standard propeller-wing configuration and wingtip propeller-wing configuration. Due to the presence of the counter-clockwise spinning propeller, the pressure difference between the upper and lower surface of the wing from wing root to the tip of the right-side blade increased when compared to the plain-wing. This can be attributed to the upwash created by the ascending blade, which increases the local angle-of-attack of the wing. This effect is palpable even when the inboard propeller is placed further away from the wing root in the wingtip propeller configuration.

The pressure difference is highest in the region directly behind the propeller and to the right of the propeller hub. Here along with the upwash, the dynamic pressure is also increased due to the additional propeller slipstream velocity. As we move to the left side of the propeller hub, the dynamic pressure remains the same but now a downwash is induced by the descending blade. This downwash reduces the local angle-of-attack and counteracts the effects of the increased dynamic pressure due to the propeller slipstream. Due to this, the pressure difference for this region seems to be even lower than that in the plain-wing configuration. This trend is similar for both inboard and outboard propellers in the standard configuration. However, the negative effects of the left-side of the inboard propeller can be seen in the wake of the outboard propeller. Similarly, the positive effect of the right-side of the outboard propeller can be seen in the wake region of the inboard propeller. This is clearly visible in figure 11, when the wake area of the inboard propeller is compared for the standard propeller configuration and wingtip propeller configuration.

For the region beyond the tip of the left blade of the outboard propeller to the wingtip, the pressure difference is reduced in the standard propeller configuration case when compared to the plain-wing case. This is due to the downwash created by the descending blade. However in the wingtip propeller configuration, only the right-side of the propeller slipstream interacts with the wing. Thus, only the positive effect of increased pressure difference is experienced by the wing due to the outboard propeller in this configuration.

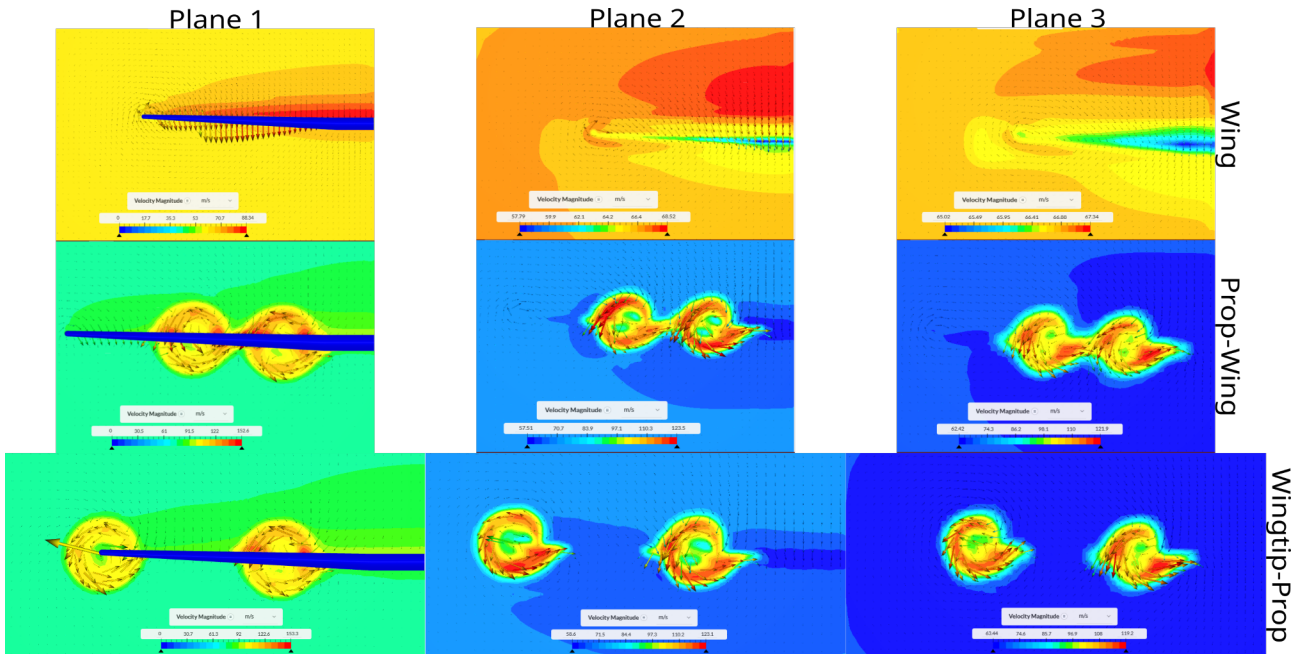


Figure 12: Velocity contours plotted at three locations along the airflow direction

In the figure 12 above, velocity contours are plotted at three different locations along the airflow direction viz. 3.43 m (Plane 1), 7.14 m (Plane 2), and 10.5 m (Plane 3) from the leading edge of the wing for all configurations. The velocity vectors shows the vorticity of the airflow in the wake region. The maximum and minimum velocities were determined for each plane and the scale was adjusted accordingly. The propeller slipstream clearly counters

the wingtip vortices in the wingtip propeller configuration. For the standard propeller configuration, the interaction between the inboard and outboard propeller slipstream can be seen.

The increased momentum of the airflow due to the propeller slipstream, also affects the wing stall behaviour by delaying it. The more energetic air tends to remain attached to the wing surface for higher angles-of-attack than normal. In the standard propeller configuration, this can be a potential problem in roll control. The stalling near the wing root should always happen before the wingtip, for roll control. As can be seen in figure 11, the propeller effects are concentrated from wing root to quarter-wingspan region. This implies that the flow will remain attached in that region for higher angles-of-attack and that the flow might separate (stall condition) at the wingtip earlier. In the case of wingtip propeller configuration, the spanwise lift distribution seems to be suitable for roll control.

Lift, Drag and Efficiency:

	Lift force (L) [N]	Drag force (D) [N]	Efficiency (L/D)
Plain-wing	79433.92	4564.71	17.4
Standard-prop config.	103242.44 (29.97%)	7166.13 (56.99%)	14.41 (-17.18%)
Wingtip-prop config.	109494.15 (37.84%)	4285.43 (-6.12%)	25.55 (46.84%)

The lift and drag force values of the last 50 timesteps were averaged-out and tabulated above. The values of lift forces corroborates the findings in previous section. The propeller slipstream indeed have a positive effect on the lift generation of the wing. The propellers in standard configuration increased the lift force on the wing by 29.97% and those in the wingtip configuration by 37.84%. The change is larger in the wingtip configuration possibly because some of the lift is recaptured at the wingtip (discussed in the previous part of the project) and also because only beneficial part of the wingtip propeller slipstream interacts with the wing.

The slipstream of the propellers in standard configuration increases the drag force on the wing by 57% when compared to the plain-wing. This can be attributed to the increased dynamic pressure due to the propeller slipstream causing the parasitic drag (specifically pressure drag) to increase. However, there is a reduction of drag force by 6.12% in the wingtip propeller configuration when compared to plain-wing. Results show a decrease of viscous drag by 88% and an increase of pressure drag by 23.5% due to the propeller slipstreams in the wingtip configuration, resulting in an overall decrease in the drag.

The aerodynamic efficiency is therefore massively improved by almost 47% when the propellers are mounted in the wingtip configuration. In the standard configuration, the positive effects of the upwash are balanced out by the negative effects of the downwash side of propeller slipstream, while in the wingtip configuration only the upwash side of the

slipstream interacts with the wing and the other part additionally counters the wingtip vortices. Hence, while the aerodynamic efficiency remains the same in the best case scenario for the standard propeller configuration, the wingtip propeller configuration ensures a significant improvement in the aerodynamic efficiency of the wing.

Bibliography

1. Aref P, Ghoreyshi M, Jirasek A, Satchell MJ, Bergeron K. Computational Study of Propeller–Wing Aerodynamic Interaction. *Aerospace*. 2018; 5(3):79. <https://doi.org/10.3390/aerospace5030079>
2. Schollenberger, M., Kirsch, B., Lutz, T., Krämer, E., & Friedrichs, J. (2024). Aerodynamic interactions between distributed propellers and the wing of an electric commuter aircraft at cruise conditions. *CEAS Aeronautical Journal*, 1-13.
3. Patil, A. & Navrátil, Jan. (2024). CFD analysis of wing-propeller interaction on the NASA X-57 Maxwell aircraft wing. *Journal of Physics: Conference Series*. 2716. 012002. 10.1088/1742-6596/2716/1/012002.
4. Savino, Alberto & Cocco, Alessandro & Zanotti, Alex & Muscarello, Vincenzo. (2022). Numerical investigation of wing-propeller aerodynamic interaction through a vortex particle-based aerodynamic solver.

Enhancing Aerodynamic Efficiency of a Wing: Winglet v/s Wingtip-Propeller

Introduction

In the first two parts of this project, we have seen how both winglet and wingtip-mounted propeller help in reducing the induced drag and therefore, improve the aerodynamic efficiency of the wing. In this last part of the project, the objective is to find out which of the two methods is better for improving the aerodynamic efficiency of a wing.

CFD Modelling and Simulation Setup

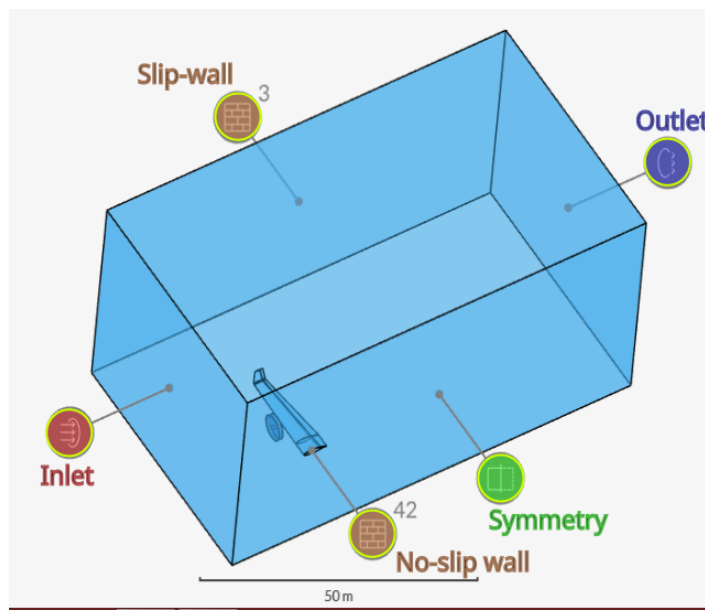


Figure 13: Simulation domain for the winglet case

The simulation modelling and setup were again done on the *Simscale* platform. The wingtip propeller configuration model from the previous part of this project was used for the wingtip propeller case, see figure 7. To model the winglet case, the winglet-wing from the first part of this project was taken and the propeller was positioned to match the inboard propeller location in the wingtip propeller case. Figure 13 shows the simulation model for the winglet case, with all the boundary conditions marked. All the mesh settings, boundary conditions and simulation setup parameters (refer the table in the second part of the project) were replicated from the second part of this project.

Results and Discussion

The simulations were run with a time-step size of 0.0001s for 5000 steps. The results below were taken from the last step at 0.5 sec.

Coefficient of Pressure (C_p):

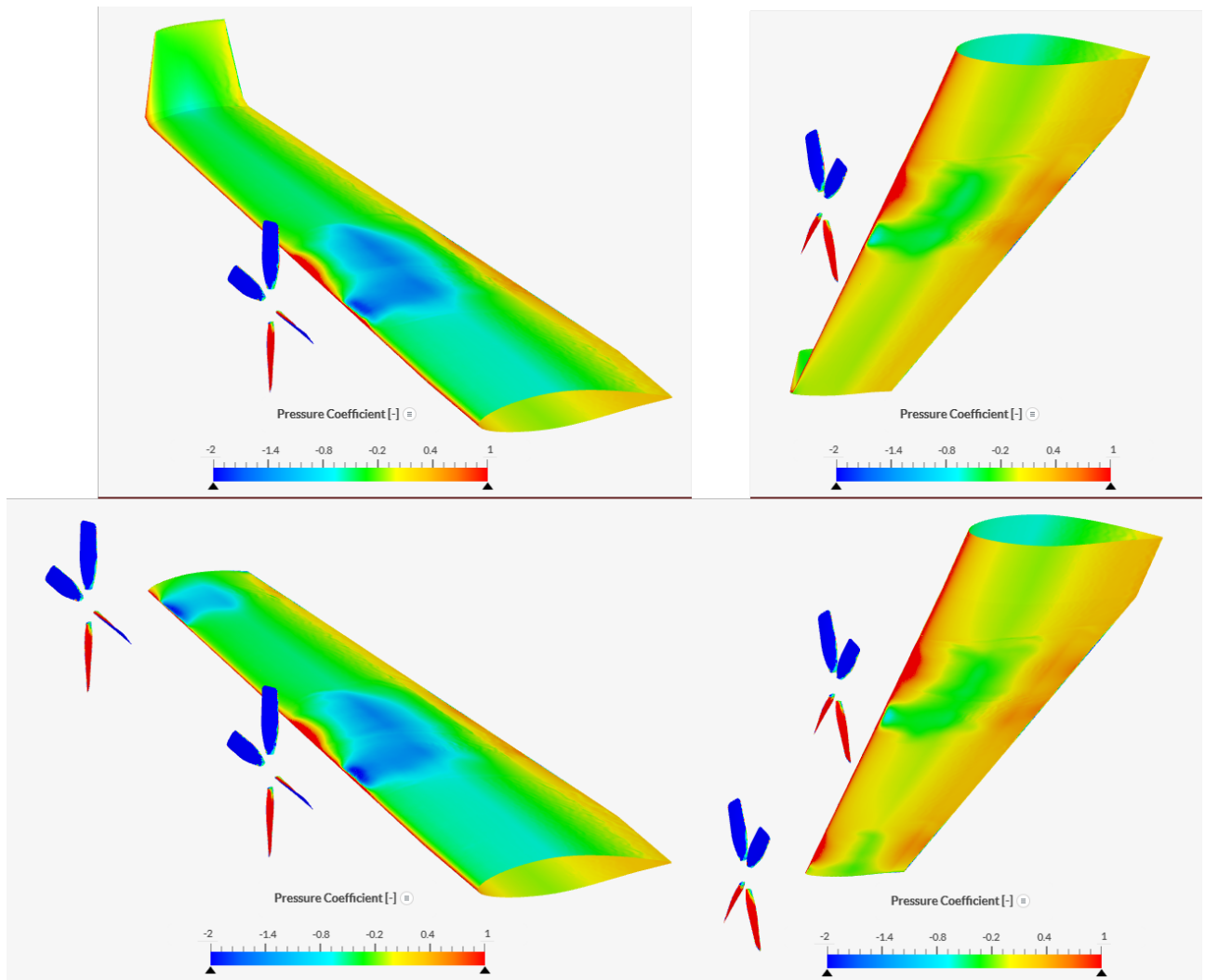


Figure 14: Pressure coefficient distributions over upper and lower wing surface for the winglet case (top) and wingtip propeller case (bottom)

Figure 14 depicts the pressure coefficient contours for both winglet case and wingtip propeller case. The inboard propeller in both the cases shows similar trends in lift distribution. At the wingtips, the distribution pattern are again reminiscent to those in first and second part of the project for the winglet case and wingtip propeller case, respectively. For a detailed discussion and analysis, please refer to the result section of the previous parts of this project.

Vorticity and Wake Velocity:

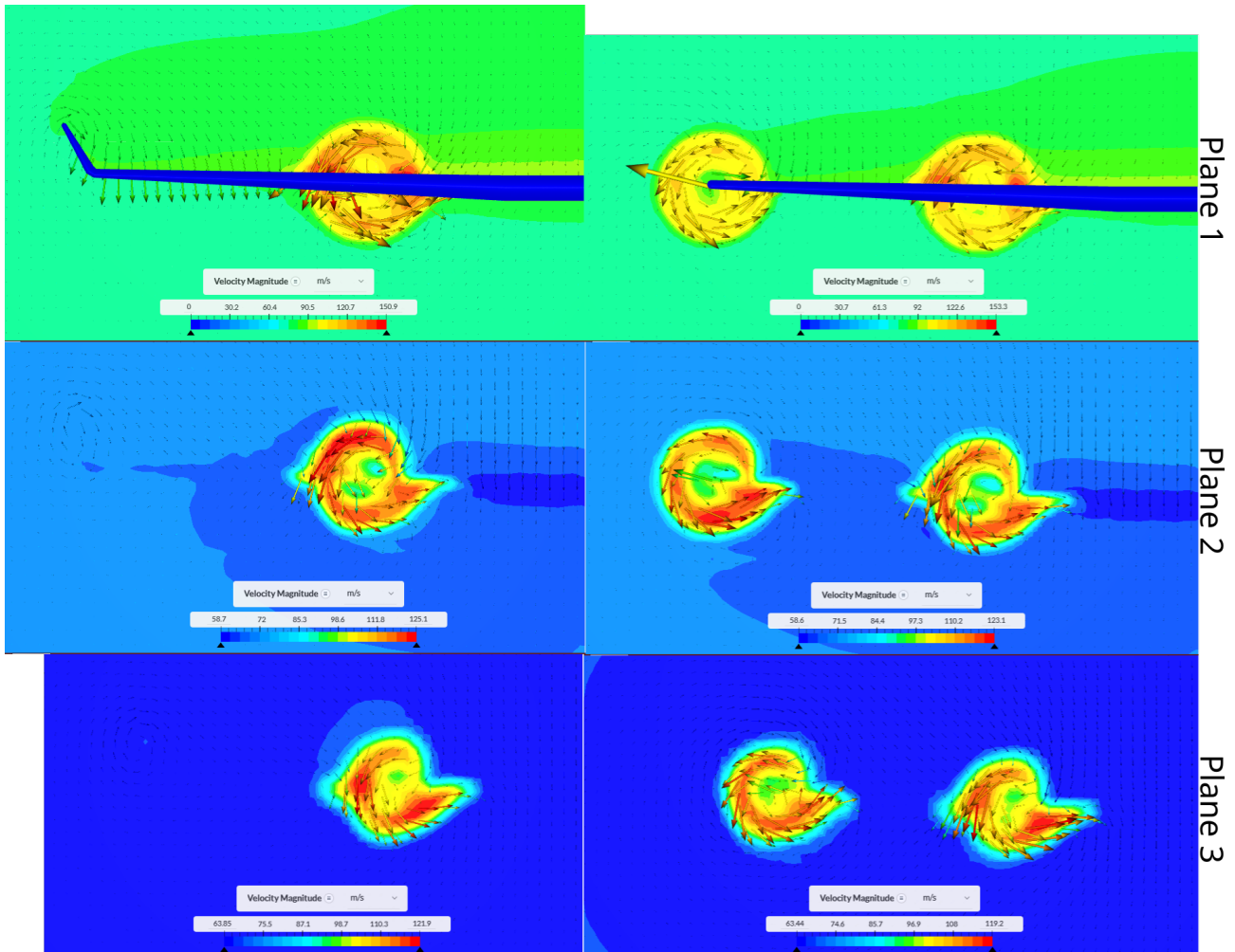


Figure 15: Velocity contours plotted at three locations along the airflow direction for winglet case (left column) and wingtip propeller case (right column)

In the figure 15 above, velocity contours are plotted at three different locations along the airflow direction viz. 3.43 m (Plane 1), 7.14 m (Plane 2), and 10.5 m (Plane 3) from the leading edge of the wing for both cases. The velocity vectors shows the vorticity of the airflow in the wake region. The maximum and minimum velocities were determined for each plane and the scale was adjusted accordingly.

Lift, Drag and Efficiency:

	Lift force (L) [N]	Drag force (D) [N]	Efficiency (L/D)
Winglet case	99275.97	5111.18	19.42
Wingtip-prop case	109494.15	4285.43	25.55

The lift and drag force values of the last 50 timesteps were averaged-out and tabulated above. It is quite evident that wingtip propeller case has better results for all the three variables. Since the inboard propeller slipstream effects are common in both cases, it is the choice between a winglet and a wingtip-mounted propeller that has made the difference in the outcomes.

While a winglet reduces the wingtip vortex strength, thereby decreasing induced drag and increasing lift force, its additional surface area and unoptimized design increases the parasitic drag. This can indeed be a disadvantage, since parasitic drag is the dominant type in cruise condition as is the case in this project. On the hand, a wingtip-mounted propeller also reduces the wingtip vortex strength but without the disadvantages of a winglet. Infact, the wingtip location exploits the upwash benefits of the propeller slipstream while escaping the negative effects of the other side of the slipstream.

As a consequence, the wingtip-mounted propeller makes the wing 31.6% more aerodynamically efficient than a winglet.